Cellular Oncology (2025) 48:219–237
https://doi.org/10.1007/s13402-024-00984-0

RESEARCH

Next-generation BCMA-targeted chimeric antigen receptor CARTemis-1: the impact of manufacturing procedure on CAR T-cell features

Belén Sierro-Martínez[1] · Virginia Escamilla-Gómez[1] · Laura Pérez-Ortega[1] · Beatriz Guijarro-Albaladejo[1] · Paola Hernández-Díaz[1] · María de la Rosa-Garrido[1] · Maribel Lara-Chica[1] · Alfonso Rodríguez-Gil[1] · Juan Luis Reguera-Ortega[1] · Luzalba Sanoja-Flores[1] · Blanca Arribas-Arribas[2,3] · Miguel Ángel Montiel-Aguilera[2] · Gloria Carmona[2] · Maria Jose Robles[4] · Teresa Caballero-Velázquez[1] · Javier Briones[5] · Hermann Einsele[6] · Michael Hudecek[6] · Jose Antonio Pérez-Simón[1] · Estefanía García-Guerrero[1]

Accepted: 9 August 2024 / Published online: 27 August 2024

Abstract

Purpose CAR therapy targeting BCMA is under investigation as treatment for multiple myeloma. However, given the lack of plateau in most studies, pursuing more effective alternatives is imperative. We present the preclinical and clinical validation of a new optimized anti-BCMA CAR (CARTemis-1). In addition, we explored how the manufacturing process could impact CAR-T cell product quality and fitness.

Methods CARTemis-1 optimizations were evaluated at the preclinical level both, in vitro and in vivo. CARTemis-1 generation was validated under GMP conditions, studying the dynamics of the immunophenotype from leukapheresis to final product. Here, we studied the impact of the manufacturing process on CAR-T cells to define optimal cell culture protocol and expansion time to increase product fitness.

Results Two different versions of CARTemis-1 with different spacers were compared. The longer version showed increased cytotoxicity. The incorporation of the safety-gene EGFRt into the CARTemis-1 structure can be used as a monitoring marker. CARTemis-1 showed no inhibition by soluble BCMA and presents potent antitumor effects both in vitro and in vivo. Expansion with IL-2 or IL-7/IL-15 was compared, revealing greater proliferation, less differentiation, and less exhaustion with IL-7/IL-15. Three consecutive batches of CARTemis-1 were produced under GMP guidelines meeting all the required specifications. CARTemis-1 cells manufactured under GMP conditions showed increased memory subpopulations, reduced exhaustion markers and selective antitumor efficacy against MM cell lines and primary myeloma cells. The optimal release time points for obtaining the best fit product were >6 and <10 days (days 8–10).

Conclusions CARTemis-1 has been rationally designed to increase antitumor efficacy, overcome sBCMA inhibition, and incorporate the expression of a safety-gene. The generation of CARTemis-1 was successfully validated under GMP standards. A phase I/II clinical trial for patients with multiple myeloma will be conducted (EuCT number 2022-503063-15-00).

Keywords CAR-T · Multiple myeloma · Manufacturing procedure · Immunophenotype monitoring · anti-BCMA

✉ Jose Antonio Pérez-Simón
josea.perez.simon.sspa@juntadeandalucia.es

✉ Estefanía García-Guerrero
egarcia-ibis@us.es

[1] Instituto de Biomedicina de Sevilla, IBiS/Hospital Universitario Virgen del Rocío/CSIC/Universidad de Sevilla, Sevilla, Spain

[2] Unidad de Producción y Reprogramación Celular de Sevilla (UPRC)-Planta CTTC Campus Virgen del Rocío de Sevilla, Red Andaluza de diseño y traslación de Terapias Avanzadas, Seville, Spain

[3] Programa doctorado Tecnología y Ciencias del Medicamento, Facultad de Farmacia, Universidad de Sevilla, Seville, Spain

[4] Unidad de Patología Comparada, Biobanco Virgen del Rocío-IBiS, Unidad de Gestión Clínica de Anatomía Patológica, Hospital Universitario Virgen del Rocío, Sevilla, Spain

[5] Servicio de Hematología, Instituto de Investigación Biomédica Sant Pau (IIB-Sant Pau), Barcelona, Spain

[6] Lehrstuhl für Zelluläre Immuntherapie, Medizinische Klinik und Poliklinik II and Medizinische Klinik und Poliklinik II, Universitätsklinikum Würzburg, Würzburg, Germany

1 Background

Chimeric antigen receptor (CAR)-T cell therapy has revolutionized the immunotherapy field with outstanding results in the treatment of several relapsed/refractory (RR) hematological malignancies. CAR-T cell therapy directed against B-cell maturation antigen (BCMA) is under clinical investigation for the treatment of multiple myeloma (MM). In the KarMMa study, Idecabtagene vicleucel (idecel) achieved an overall response rate (ORR) of 73% and the median progression-free survival (PFS) was 8.8 months [1]. Ciltacabtagene autoleucel (cilta-cel) showed an ORR of 97.9% at 27.7 months with a median PFS of 34.9 months in the CARTITUDE-1 study [2–5]. However, although real-world evidence remains limited in BCMA-directed CAR-T therapy, idecel and cilta-cel have shown 1-year progression rates of 60% and 33%, respectively, in clinical trials [1, 3, 6]. Therefore, relapse ultimately remains common with all approved anti-BCMA CAR-T products [7]. In this sense, several limitations have been identified that may explain the ultimate relapse of patients. The heterogeneity of BCMA expression levels in patients, the presence of soluble BCMA in blood, on-/off-tumor toxicity, the lack of CAR-T cell persistence, and poor quality of T-cell products are some of the limitations that may affect CAR-T cell therapy in MM [8]. The development of next-generation CAR-T cells is mandatory to overcome restrictions to CAR-T efficacy observed in the real-world setting.

We present a novel academic BCMA CAR-T product (CARTemis-1) developed following a rational design for enhanced antitumoral efficacy against plasma cells. Remarkably, CARTemis-1 is not hindered by soluble BCMA and contains a safety-gene marker. CARTemis-1 shows potent antitumor efficacy in preclinical models, both in vitro and in vivo, and its manufacture has been validated under GMP conditions. Importantly, little attention has been given to what happens during ex-vivo expansion and maintenance of CAR-T cells and the effect of the manufacturing process on the dynamics of the immunophenotype of cell products. In this study, CAR-T cells produced under GMP conditions were monitored during the manufacturing process, and immunophenotypic and functional characterization were performed to identify the optimal time for expansion. In addition, the dynamics of CAR-T cells during the manufacturing process, and how manufacturing process impacts CAR-T cell features and quality were assessed. A phase I/II clinical trial for patients with multiple myeloma will be conducted (EuCT number 2022-503063-15-00).

2 Methods

2.1 CAR gene construct and design

A codon-optimized single chain variable fragment (scFv) comprising the variable heavy (VH) and variable light (VL) chains of the anti-BCMA mAb BCMA30 [9] (separated by two different (G4S)3 linkers, were synthesized (GeneArt, Regensburg, Germany) and fused to a different spacer and a transmembrane domain, a 4-1BB_CD3ζ signaling module, a T2A element and a safety-gene composed of a truncated epidermal-growth -factor-receptor (EGFRt) in an epHIV7 lentiviral vector backbone.

2.2 In vitro studies with CARTemis-1

Cytotoxic activity was analyzed in a bioluminescence-based assay using firefly luciferase (ffluc)-transduced target cells and distinct effector-to-target cell (E: T) ratios at 4 h post-coculture. Assay was performed with 5×10^3 target cells/well with effector T cells at various E: T ratios in triplicate wells. Specific lysis was calculated using a standard formula [10]:

$$\%\ specific\ lysis = \left(\frac{Mean\ bioluminiscence\ of\ target\ cells\ -\ Mean\ bioluminiscence\ of\ coculture}{Mean\ bioluminiscence\ of\ target\ cells}\right) * 100$$

Proliferation of T cells was analyzed by carboxyfluorescein succinimidyl ester (CFSE) (Biolegend, Ref: 423801) dye dilution after 72 h of coculture with target cells (E: T ratio of 4:1). IFN-γ, IL-2 and GM-CSF secretion in supernatants obtained after 24 h of coculture of T cells with target cells (E: T ratio of 4:1) were measured by enzyme-linked immunosorbant assay (ELISA) (Biolegend). Assay was performed in triplicate wells with 5×10^3 target cells per well. Recombinant soluble BCMA protein was obtained from R&D Systems (R&D Systems, Ref: ATM193). Primary myeloma cells were obtained from bone-marrow samples from patients with multiple myeloma at the time of diagnosis and were isolated using MACSprep™ Multiple Myeloma CD138 MicroBeads Human from Miltenyi Biotec (Ref: 130-111-744) and an AutoMACS Pro Separator (Miltenyi Biotec).

2.3 In vivo studies with CARTemis-1

The University of Würzburg Institutional Animal Care and Use Committee and the Institutional Animal Care and Use Committee at the Institute of Biomedicine in Seville approved all animal procedures. Six-to-eight-week-old NSG (NOD-scid IL2rγnull) mice were obtained from Charles River (Sulzfeld, Germany). Tumor cells, PBMCs,

or CAR-T cells were inoculated via the tail injection vein, and animals were randomly allocated to the treatment groups. Specific methods used for the three different mouse models are described in Supplementary Material.

2.4 GMP-manufacture of CARTemis-1

Apheresis products from healthy donors were connected to CliniMACS Prodigy system (Miltenyi Biotec, Germany). CD4+/CD8+ white blood cells were selected using coated-magnetic beads (Miltenyi Biotec, Ref: 200-070-213, and Ref: 200-070-215, respectively). A total of 1×10^8 cells were used to initiate cell culture with TexMACs (Miltenyi Biotec, Ref: 170-076-306) supplemented with IL-7 and IL-15 (Miltenyi Biotec, Ref: 170-076-184, and Ref: 170-076-114, respectively). Cells were activated using TransACT (Miltenyi Biotec, Ref: 200-076-204) and transduced at a multiplicity of infection of 5 at day 2 post-activation. In vitro cytotoxicity, cytokines, and quality control assays were performed on days 8, 9, and 10 post activation. CARTemis-1 products were frozen according to dose and thawed to perform stability studies at 6 and 12 months after cryopreservation. A graphical summary of GMP-manufacture of CARTemis-1 in CliniMACS Prodigy is included in Supplementary Material. Additional information regarding quality controls according to GMP standards is described in Supplementary Material.

2.5 Statistical analysis

Statistical analyses were performed using Prism software v6.07 (GraphPad, San Diego, California). Unpaired and paired t-tests were used to analyze data from in vitro experiments. P values <0.05 were considered to indicate statistical significance. Survival curves were analyzed using Log-rank (Mantel-cox) test. The measurements per group are presented as the means and standard deviations. When the qq plots showed no normally distributed data and due to the small sample size, nonparametric Mann-Whitney U tests were used as significance tests for comparing the measurements between groups.

3 Results

3.1 Rationally designed next-generation anti-BCMA CAR-T (CARTemis-1) shows potent target recognition and no susceptibility to soluble BCMA inhibition

CAR-T cell design including scFv antigen binding domain, costimulatory domain or spacer region have shown to impact CAR-T functionality and clinical outcome. Therefore, two different versions of a new anti-BCMA CAR-T cell construct were synthesized (short and long, Fig. 1a). The short version consists of the IgG4 hinge domain (12 AA), and the long version contains the IgG4 hinge-CH2-CH3 domain (229 AA). Both CAR construct versions contain the safety-gene EGFRt as a transduction marker. CAR expression according to the EGFRt marker or the molecule that recognizes the BCMA-CAR in the membrane was equivalent (Fig. 1b); therefore, the EGFRt marker was used as a detection reagent for CAR-T cells. No differences in T-cell transduction were observed between the two versions (25.08% CAR+ in the short version vs. 23.98% in the long version, $p=0.7771$) (Supplementary Fig. 1). However, the long version of the anti-BCMA CAR-T showed significantly greater antimyeloma function than the short version at all studied ratios (Fig. 1c e.g., an effector-to-target ratio (E: T) 5:1, $p<0.001$). Similarly, the release of IFN-γ by CD8+ CAR+ T cells was significantly greater for long spacer than for short spacer (Fig. 1d, $p<0.05$). Consistently, the long version of our anti-BCMA CAR-T cell construct (CARTemis-1) was selected for further studies. These results demonstrate that the incorporation of the safety-gene EGFRt into the CARTemis-1 structure can be used as a monitoring marker. Besides, the long version of CARTemis-1 shows enhanced tumor recognition with increased anti-tumoral potency.

The extracellular portion of membrane-bound BCMA can be shed from myeloma cells to release a shorter, soluble BCMA (sBCMA) protein isoform. Soluble BCMA protein was quantified in the serum of patients with multiple myeloma at different disease stages, and doses up to 10 times greater than the amount of recombinant soluble BCMA protein were used for in vitro studies ($n=10$ patients, Supplementary Fig. 2). We confirmed that the antitumor activity of CARTemis-1 was not diminished in the presence of the highest concentration of recombinant sBCMA protein (150 ng/mL) (e.g., an E: T ratio of 5:1, MM.1 S, $p=0.7$, Fig. 1e). In addition, we analyzed the percentage of activated CARTemis-1 cells in the presence of recombinant sBCMA (and absence of tumor) to determine whether sBCMA could cause nonspecific activation of CAR T-cells. For that, CD4+/CD8+ CARTemis-1 cells were cultured using increasing doses of recombinant sBCMA protein, and the percentage of CD25+/CD69+ T lymphocytes was analyzed. No differences in the percentage of CD25+/CD69+ T-cells were observed when CARTemis-1 cells were cultured with or without sBCMA (Fig. 1f, e.g., CD4 + cells, 0 vs. 150 ng/mL $p=0.996$; CD8 + cells, 0 vs. 150 ng/mL $p=0.5813$). Furthermore, as an indication of cell activation, we investigated the release of IFN-γ. IFN-γ secretion was similar when CARTemis-1 cells were cultured with or without sBCMA (e.g., CD4 + cells, 0 VS 150 ng/mL $p=0.9990$; CD8+ cells, 0 vs. 150 ng/mL $p=0.5821$) (Fig. 1f). These

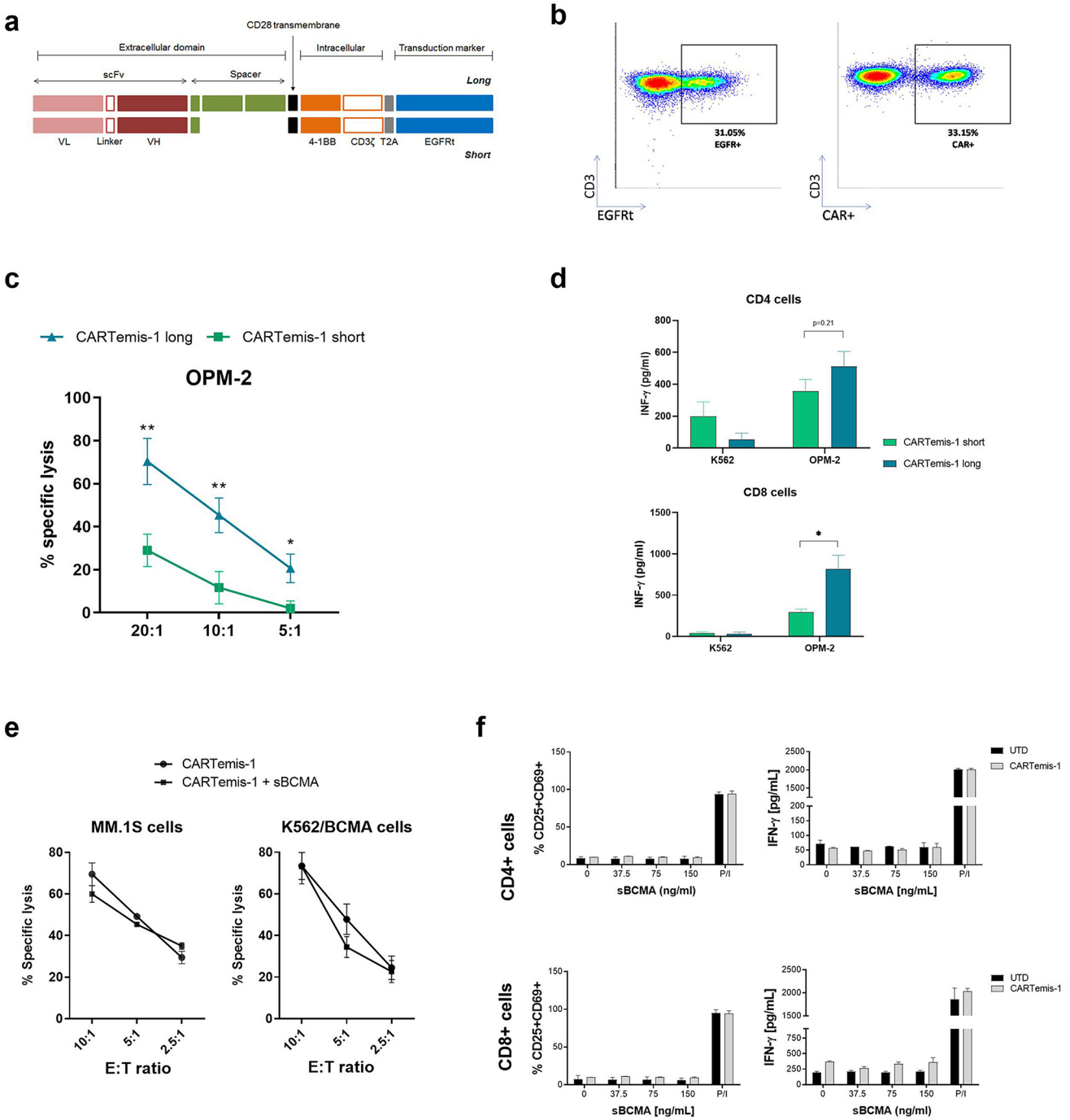

Fig. 1 Long version of anti-BCMA CAR-T (CARTemis-1) shows increased antitumor potency and is not affected by soluble BCMA. **a** Schema of the anti-BCMA CAR-T genes comparing the long version *(top)* with the short version *(bottom)*. EGFRt was incorporated into the CAR gene design as transduction marker. **b** Flow cytometry plot of the identification of CAR+ T cells with anti-EGFR *(left)* or with anti-BCMA CAR-T cell detection reagent (*right*). **c** Tumor specific lysis of OPM-2 or K562 cells at different E: T ratios with long and short anti-BCMA CAR-T cells at 4 h post-coculture. (E: CD3+T cells, T: tumor cell lines). Assay was performed in triplicate wells with 5,000 target cells per well ($n=3$ biological replicates depicted). **d** Cytokine release of IFN-γ of CD4+ *(top)* and CD8+ *(bottom)* CAR-T cells against BCMA+tumor cells of both versions of anti-BCMA CAR-T cells at 24 h post-coculture. Assay was performed in triplicate wells with 5,000 target cells per well ($n=3$ biological replicates depicted). **e** Tumor specific potency of CARTemis-1 against myeloma cell lines (MM.1 S or K562/BCMA) with or without sBCMA (150ng/mL) in the media at 4 h post-coculture. Assay was performed in triplicate wells with 5,000 target cells per well ($n=3$ biological replicates depicted). **f** Activation (CD25+CD69+) and cytokine release (IFN-γ) levels of CD4+ *(top)* and CD8+ *(left)* CARTemis-1 cells in the presence of soluble BCMA (150ng/mL) in the media at 24 h post-incubation. Assay was performed in triplicate wells with 5,000 target cells per well. One representative experiment is depicted from $n=2$ independent biological replicates performed. Depicted are mean values + standard deviation. *P*-values between the indicated groups were calculated using unpaired T-test. $*p<0.05$ $**p<0.01$, $***p<0.001$

results show that soluble BCMA protein does not interfere with the effectiveness of CARTemis-1.

3.2 CARTemis-1 shows potent efficacy against myeloma cells both in vitro and in vivo

CARTemis-1 was then validated at the preclinical level using in vitro and in vivo models. We first evaluated the antitumor activity of CARTemis-1 versus control activated untransduced (UTD) T cells from the same donor. CARTemis-1 specifically killed BCMA+ MM cell lines (MM.1S, OPM-2 and K562/BCMA) without affecting the BCMA- control cell line (K562) (Fig. 2a). Control-activated untransduced T cells showed weak and indistinguishable cytotoxicity against BCMA+ or BCMA- cells. (Supplementary Fig. 3). Quantitative cytokine analysis revealed that CARTemis-1 induces IFN-γ and IL-2 release in a target-specific manner (e.g., IFN-γ secretion of CARTemis-1 cells against OPM-2 1332.8 pg/mL vs. 16.26 pg/mL from UTD, $p < 0.0001$ in CD4 + compartment; IFN-γ secretion of CARTemis-1 cells against OPM-2 203.19 pg/mL vs. 16.4 pg/mL from UTD, $p = 0.02$) (Fig. 2b). Cocultures between CFSE-labeled CARTemis-1 cells and BCMA-expressing target cells were performed. After 72 h, CD4+/CD8+ CARTemis-1 cells showed a potent and specific proliferative capacity (Fig. 2c and d).

Finally, we analyzed the antitumor efficacy of CARTemis-1 in a systemic BCMA+ MM xenograft model (NSG/MM.1S-ffLuc). First, high levels of soluble BCMA were confirmed in the MM mouse model compared with the control mice (without tumor inoculation) (mean sBCMA levels in MM.1S inoculated mice was 2384.02 pg/mL vs. 0 pg/mL in control mice, $p < 0.0001$) (Fig. 2e). In a second in vivo experiment, a potent antitumor effect was mediated by a single dose of CD4+ and CD8+ CARTemis-1 cells. These cells rapidly eradicated myeloma cells in all treated mice ($n = 8$), whereas the mice receiving control untransduced T-cells ($n = 7$) exhibited progressive, deleterious myeloma. Follow-up by tumor bioluminescence detection revealed tumor eradication in 100% of the treated mice at one-week post infusion, while the control group (treated with an equal dose of untransduced T-cells from the same donor) exhibited 100% mortality due to tumor progression (Fig. 2f). Average radiance of mice infused with untransduced T cells was significantly higher than mice infused with CARTemis-1 at days 21, 28 and 41 post infusion (e.g. 7.56×10^6 p/s/cm²/sr in mock vs. 2191 p/s/cm²/sr in CARTemis-1, $p = 0.0092$) (Supplementary Fig. 4). We obtained bone marrow from mice in each treatment group on day 48 post myeloma inoculation and performed flow cytometric analysis which confirmed complete clearance of MM.1S myeloma cells after treatment with CARTemis-1 (Fig. 2g). Kaplan-Meier curves revealed 100% survival in mice treated with CARTemis-1, while all mice receiving UTD cells were euthanized due to disease progression (Fig. 2h). In summary, our data demonstrate that CARTemis-1 is highly potent in vitro and in vivo against myeloma cells without reducing its antimyeloma activity in the presence of sBCMA in vivo.

3.3 Characterization and optimization of the manufacturing protocol

Manufacturing protocol is critical for obtaining the optimal CAR-T cell product in a clinical setting with the best fitness to induce prolonged responses. Two different expansion protocols were tested. CARTemis-1 was expanded for 21 days in the presence of either IL-2 or IL-7/IL-15 cytokines. Similar CAR-T cell transduction rates were observed with both protocols (e.g., a median of 35.92% vs. 39.83% for IL-2 vs. IL-7/IL-15 for CD4+ cells) ($n = 8$) (Fig. 3a). However, CARTemis-1 cell expansion was significantly increased with IL-7/IL-15 (e.g., CD4+ cells on day 15 of expansion 3.04×10^7 vs. 1.59×10^7 cells with IL-7/IL-15 vs. IL-2, respectively, $p = 0.0047$) (Fig. 3b).

Immunophenotypic characterization was performed to assess T-cell subpopulations, activation, and exhaustion by comparing both protocols ($n = 8$). The gating strategy used to determine different T-cell subpopulations (naïve, stem cell memory, central memory, effector memory, and effector) is shown in Supplementary Fig. 5. CD4+ CAR-T cells showed significantly increased accumulation of naïve and stem cell memory (TSCM) population (e.g., 53.01% vs. 46.26% of TSCM cells in the IL-7/IL-15 group vs. IL-2 group on day 21, respectively, $p = 0.0415$) and a reduced proportion of central memory (CM) and effector memory (EM) cells in the presence of IL-7/IL-15 (e.g., 13.83% vs. 25.99% of CM in the IL-7/IL-15 group vs. IL-2 group on day 15, $p = 0.0029$) (Fig. 3c). The proportion of effector population (EMRA) showed a tendency to a decrease at the end of the expansion protocol in the presence of IL-7/IL-15 compared to IL-2 group (13.41% vs. 17.20% for IL-7/IL-15 vs. IL-2, respectively, $p = 0.0836$) (Fig. 3c). Compared with those in the presence of IL-2, the proportion of CM CD8+ CAR-T cells showed a tendency to a decrease on days 8 and 15 (e.g., 4.3% vs. 10.52% on day 15 in IL-7/IL-15 vs. IL-2 groups respectively, $p = 0.0778$ (Fig. 3c). Although there seems to be a global tendency toward a reduced proportion of CM with IL-7/IL-15 in CD4+/CD8+ CAR-T cells, this trend was lost at the end of the expansion protocol (day 21). Notably, the percentages of both naïve and TSCM cells were significantly greater in the CD8+ CAR-T cells expanded with IL-7/IL-15 (40.34% vs. 33.8%, respectively; $p = 0.0219$) (Supplementary Fig. 6). T-cell activation was also analyzed during expansion, and

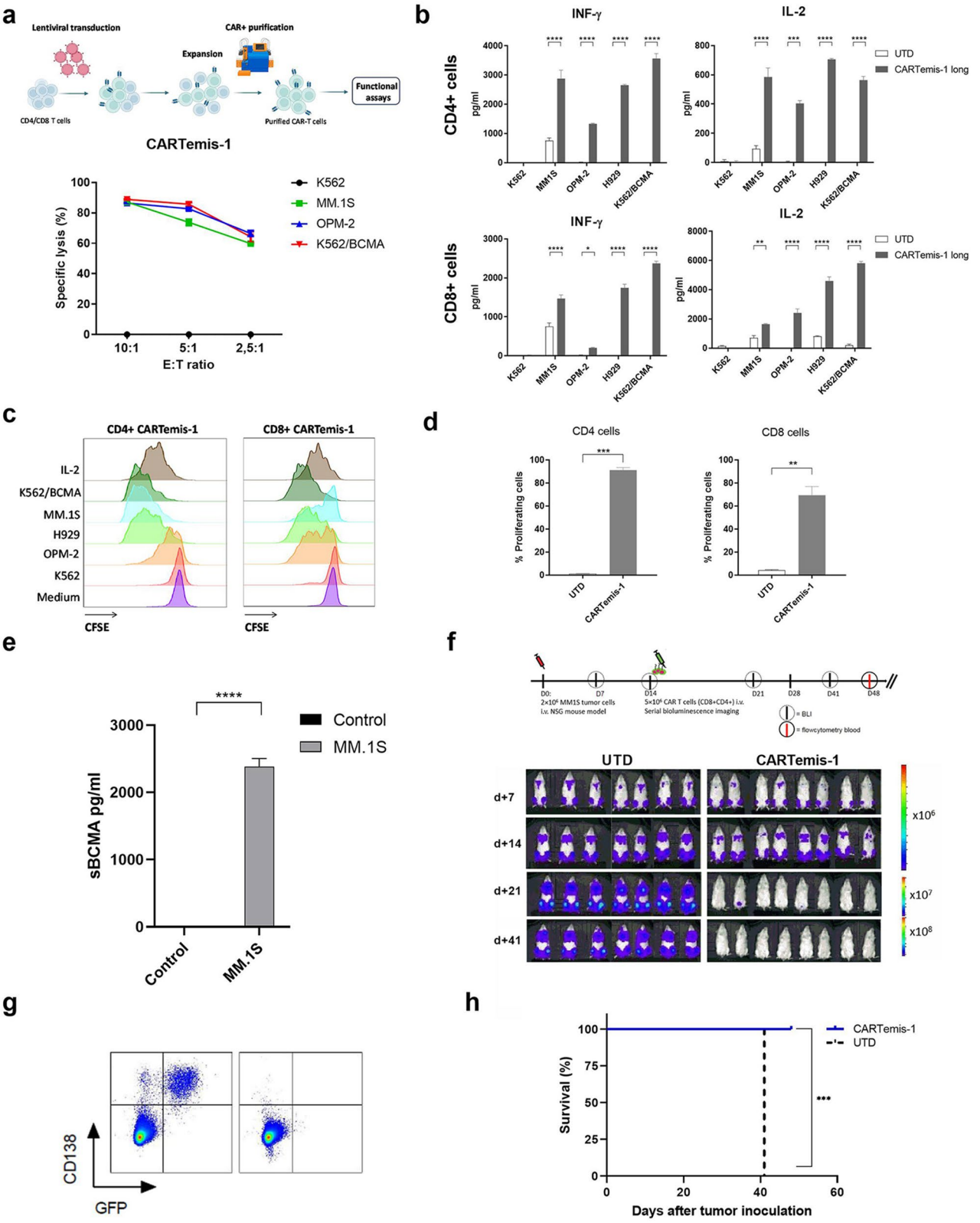
a
Lentiviral transduction
CAR+ purification
Expansion
CD4/CD8 T cells
Purified CAR-T cells
Functional assays
CARTemis-1
Specific lysis (%)
E:T ratio
10:1
5:1
2,5:1
K562
MM.1S
OPM-2
K562/BCMA
b
INF-γ
IL-2
CD4+ cells
CD8+ cells
pg/ml
UTD
CARTemis-1 long
c
CD4+ CARTemis-1
CD8+ CARTemis-1
IL-2
K562/BCMA
MM.1S
H929
OPM-2
K562
Medium
CFSE
d
CD4 cells
CD8 cells
% Proliferating cells
UTD
CARTemis-1
e
sBCMA pg/ml
Control
MM.1S
f
D0:
2×10⁶ MM1S tumor cells
i.v. NSG mouse model
D7
D14
5×10⁶ CAR T cells (CD8+CD4+) i.v.
Serial bioluminescence imaging
D21
D28
D41
D48
= BLI
= flowcytometry blood
UTD
CARTemis-1
d+7
d+14
d+21
d+41
x10⁶
x10⁷
x10⁸
g
CD138
GFP
h
Survival (%)
Days after tumor inoculation
CARTemis-1
UTD

Fig. 2 Preclinical validation of CARTemis-1 shows efficient antitumoral potency against myeloma cells both in vitro and *in vivo*. Purified CARTemis-1 (100% CAR+cells) was validated in vitro and in vivo at preclinical level. **a** CD4+and CD8+cells were obtained from buffy coats of healthy donors and transduced with lentiviral vectors, expanded, and purified using AutoMACs Pro to obtained 100% CAR+cells. Antitumor cytotoxicity of purified CARTemis-1 against myeloma cell lines (MM.1S, OPM-2, K562/BCMA) at different E: T ratios at 4 h post-coculture (E: CAR+T cells, T: tumor cell lines). Assay was performed in triplicate wells with 5,000 target cells per well. One representative experiment is depicted from $n=3$ independent biological replicates performed. **b** Cytokine release of CD4+ *(top)* and CD8+ *(bottom)* purified CARTemis-1 cells against MM cell lines (MM.1S, OPM-2, K562/BCMA) at 24 h post-coculture. Assay was performed in triplicate wells with 5,000 target cells per well. One representative experiment is depicted from $n=3$ independent biological replicates performed. **c** Histogram plots of proliferation assay of CD4+ *(left)* and CD8+ *(right)* purified CARTemis-1 cells after coculture with MM cell lines (MM.1S, OPM-2, K562/BCMA) at 72 h post-coculture. **d** Quantification of the proliferation assay of CD4+ *(left)* and CD8+ *(right)* CARTemis-1 cells or control activated untransduced T cells against K562/BCMA cells. Assay was performed in triplicate wells with 5,000 target cells per well ($n=3$ biological replicates depicted). **e** Soluble BCMA protein levels in the serum of non-inoculated control mice or mice inoculated with multiple myeloma cells. *P*-values between the indicated groups were calculated using unpaired T-test. **f**In vivo antitumor potency of CARTemis-1 is depicted. NSG mice were inoculated with 2×10^6 MM.1 S cells. After 14 days, mice were inoculated with 5×10^6 CARTemis-1 cells (CD4+/CD8+). **g** Flow cytometry analysis of the bone marrow and bioluminescence were measured until 48 days post-inoculation. **h** Survival curves of mice treated with untransduced T cells compared to CARTemis-1. Log-rank (Mantel-cox) test was used. Results from one out of two independent experiments from different healthy donors is shown. $*p<0.05$ $**p<0.01$, $***p<0.001$

compared with the IL-2 protocol, the IL-7/IL-15 protocol significantly increased CD25+expression on day 21, in both CD4+ (85.23% vs. 23.81%, respectively; $p<0.0001$) and CD8+CAR-T cells (76.9% vs. 12.33%, respectively; $p=0.0269$) (Fig. 3d). Remarkably, CD25+expression was dramatically reduced in CD4+and CD8+CAR-T cells during the manufacturing process with the IL-2 protocol (e.g., CD4+cells on day 8: 83.7% vs. day 21: 18.29%, $p<0.0001$) (Fig. 3d and Supplementary Fig. 7). CD69 levels were also significantly increased in CD8+CAR-T cells in the presence of IL-7/IL-15 (37.77% vs. 20.32% on day 21 in the IL-7/IL-15 group vs. IL-2 group, respectively; $p=0.0001$) (Fig. 3e). Moreover, the expression of coinhibitory molecules such as PD-1 and LAG-3 was monitored during the manufacturing process. PD-1 and LAG-3 expression was significantly lower in CD4+CAR-T cells and tended to be a slightly lower in CD8+CAR-T cells expanded with IL-7/IL-15 than in those expanded with IL-2 (0.55 vs. 1.38%, $p=0.0338$ for CD4+cells and 0.32 vs. 1.12%, $p=0.1633$ for CD8+cells, respectively) (Fig. 3f). In summary, our data demonstrate that CARTemis-1 expansion with IL-7/IL-15 results in greater proliferation, less differentiation, and lower exhaustion than does the IL-2 protocol.

By focusing on the dynamics of the CARTemis-1 immunophenotype during the manufacturing process (from day 0 to day 21) using the IL-7/IL-15 protocol, we identified the optimal time for ex vivo expansion and, therefore, the optimal release time considering CAR-T cell product quality. CAR-T cell expansion did not increase between days 15 and 21 postactivation in either the CD4+or CD8+compartments (Fig. 3b). Immunophenotypic characterization of CAR-T cells during the 21 days of cell culture revealed the same trend in all healthy donors (Supplementary Figs. 7–8). T-cell subpopulations from day 0 to day 21 showed a dynamic increase in TSCM and effector cells and a reduction in naïve and central memory during the manufacturing protocol for the CD4+and CD8+populations (Supplementary Fig. 8). The CD25+marker was maintained in both CD4+and CD8+CAR-T cells cultured in the presence of IL-7/IL-15 (Supplementary Fig. 9). PD-1/LAG-3 expression in CD4+cells significantly increased on day 8 post activation and then decreased until days 15–21 (Supplementary Fig. 9). Based on these preclinical results, the optimal time to obtain the best-fitness product for clinical translation was 10 days of ex vivo expansion for clinical translation.

3.4 CARTemis-1 cells can be successfully manufactured under GMP conditions with increased memory subpopulations and reduced exhaustion markers

CARTemis-1 was generated under GMP conditions from leukapheresis from three healthy donors as a clinical validation process. Manufacturing process, including IL-7/IL-15 cytokines and 10 days of ex vivo expansion, was performed according to our previous preclinical data. Finally, CARTemis-1 cells were cryopreserved at the requested CAR-T cell dose. CAR-T cell transduction, cell viability, cell expansion, and CAR-T cell immunophenotyping were analyzed during the manufacturing process and at the final cryopreserved CAR-T cell product. In Table 1, the release criteria of all three manufacturing processes are depicted. CAR-T cell transduction was similar in all lots with a mean of 34.43% for the final cryopreserved product (Fig. 4a). CAR-T cell expansion occurred in all lots and CAR-T cell dose was achieved via all three manufacturing processes (Fig. 4b; Table 1). CAR-T cells were monitored during the manufacturing process in the CliniMACS Prodigy, and T-cell cluster formation was observed to confirm activation (Fig. 4c). CAR-T cell immunophenotyping was performed throughout the manufacturing process to study CAR-T cell fitness and establish the optimal ex-vivo expansion time. T-cell subpopulation analyses revealed an increased proportion of TSCM and CM at the final CARTemis-1 product in all lots (Fig. 4d). T-cell activation (CD25+and CD69+)

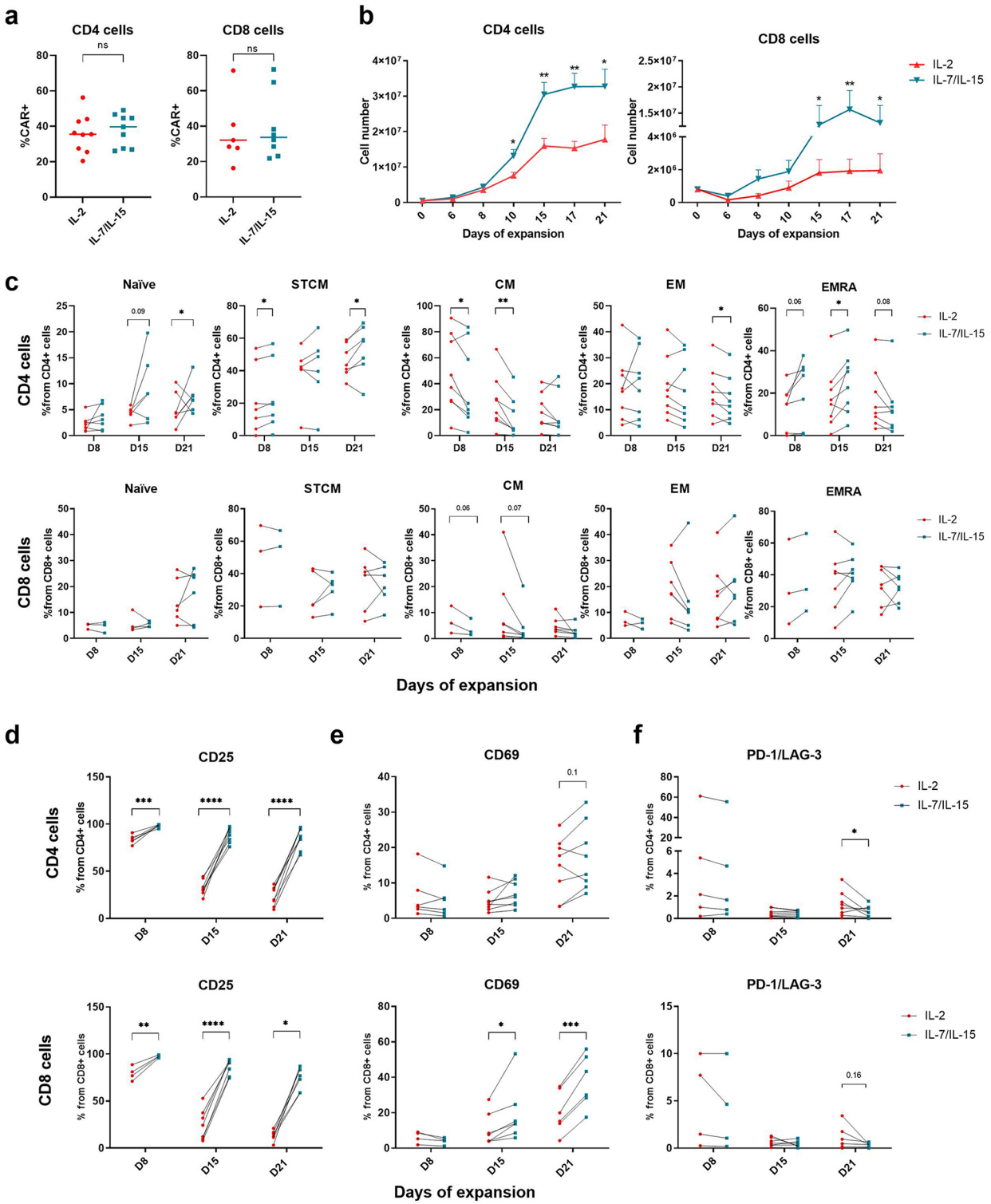

Fig. 3 IL-7/IL-15 expansion protocol increases CARTemis-1 proliferation in vitro and generates a less differentiated, more activated, and less exhausted product. **a** CAR-T cell transduction in CD4+ *(left)* and CD8+ *(right)* CARTemis-1 with IL-7/IL-15 and IL-2. **b** CARTemis-1 cell proliferation of CD4+ *(left)* and CD8+ *(right)* with IL-7/IL-15 and IL-2 ($n = 8$ biological replicates). Depicted are mean values + standard error of the mean. **c** Immunophenotypic characterizationof T cell subsets (naïve, stem cell memory, central memory, effector memory and effector) of CD4+ *(top)* and CD8+ *(bottom)* CARTemis-1 cells expanded with IL-7/IL-15 or IL-2 at different days of expansion. **d** Immunophenotypic characterization of the levels of activation CD25+. **e** CD69+ and exhaustion. **f** PD1+/LAG3+ of CD4+ *(top)* and CD8+ *(bottom)* CARTemis-1 cells expanded with IL-7/IL-15 or IL-2 at different days of expansion. *P*-values between the indicated groups were calculated using paired T-test. $*p < 0.05$ $**p < 0.01$, $***p < 0.001$, $****p < 0.0001$

Table 1 CARTemis-1 clinical product release criteria and specifications

Specification	Release criteria	2108-CARTemis1	2111-CARTemis1	2202-CARTemis1
RCL	Negative (<2 copies)	*D8: Negative (0 copies) *D9: Negative (0 copies) *D10: Negative (0 copies)	*D8: Negative (0 copies) *D9: Negative (0 copies) *D10: Negative (0 copies)	*D8: Negative (0 copies) *D9: Negative (0 copies) *D10: Negative (0 copies)
Viability	≥70%	*D8: 92.1% *D9: 94.5% *D10: 93.7%	*D8: 90.1% *D9: 90.5% *D10: 91.5%	*D8: 88.1% *D9: 92.8% *D10: 94.2%
%CAR+ (EGFR+ from CD3+)	≥10%	*D8: 41.0% *D9: 35.2% *D10: 30.3%	*D8: 42.0% *D9: 31.0% *D10: 34.2%	*D8: 50.6% *D9: 46.8% *D10: 36.9%
Proposed CAR-T cell dose	Assumed 70 kg patient weight Dose (0.5×10^6-6×10^6 cells/kg): 35×10^6-420×10^6 CAR+ anti-BCMA T cells ±20%	35×10^6 CAR+ cells anti BCMA	Dose 1: 140×10^6 CAR+ cells anti BCMA Dose 2: 280×10^6 CAR+ cells anti BCMA	70×10^6 CAR+ cells anti BCMA
Final viable CAR-T cells obtained ($x10^6$)	NA	1465	948	1668
Endotoxins (patient weight 70 Kg)	3.5 EU/mL	<0.5 EU/mL	<0.5 EU/mL	<0.5 EU/mL
Mycoplasma	Absence	Absence	Absence	Absence
Sterility	Sterile (Negative Growth)	Sterile	Sterile	Sterile
Vector Copy Number or Virus Copy Number (VCN)	<10 copies	0.97	1.51	0.87
Biological activity (Cytotoxicity or potency)	MM.1 S or OPM-2 tumor cell lysis ≥20% (10:1 effector to target ratio at 24 h)	CARTemis-1 /MM.1 S *D8: 92.77% *D9: 87.21% *D10: 91.55% CARTemis-1 / OPM-2 *D8: 72.65% *D9: 95.47% *D10: 99.06%	CARTemis-1 /MM.1 S *D8: 93.31% *D9: 89.16% *D10: 92.92% CARTemis-1 / OPM-2 *D8: 89.42% *D9: 73.37% *D10: 84.04%	CARTemis-1 /MM.1 S *D8: 87.18% *D9: 51.22% *D10: 85.05% CARTemis-1 / OPM-2 *D8: 87.62% *D9: 87.26% *D10: 73.99%
Viral adventitious agents	Negative	Negative	Negative	Negative
Karyotype	Normal	Normal	Normal	Normal
Residual analysis of viable lentiviruses	ELISA analysis with result of detection of descending or non-reactive levels of p24 protein in successive cultures of permissive cell lines (Jurkat and HEK293T) with supernatant from anti-BCMA CAR-T cells. Absence of %CAR (EFGR+) in permissive cells (Jurkat and HEK293T).	– Descending level of p24, becoming non-reactive from the 2nd culture of Jurkat and HEK293T. – Absence of CAR marker (EFGR)	– Descending level of p24, becoming non-reactive from the 2nd culture of Jurkat and HEK293T. – Absence of CAR marker (EFGR)	– Descending level of p24, becoming non-reactive from the 2nd culture of Jurkat and HEK293T. – Absence of CAR marker (EFGR)
Infective HIV (gp120)	Absence	Absence	Absence	Absence
Gram	Absence of Gram + and Gram − bacteria	Absence of G+ and G− bacteria	Absence of G+ and G− bacteria	Absence of G+ and G− bacteria

Data from 3 independent batches produced is shown. *RCL* replicative competent lentivirus, *D8* day 8 of expansion, *D9* day 9 of expansion, *D10* day 10 of expansion, *NA* not applicable, *EU* endotoxins units, *HIV* human immunodeficiency virus, *ELISA* enzyme-linked immunosorbent assay

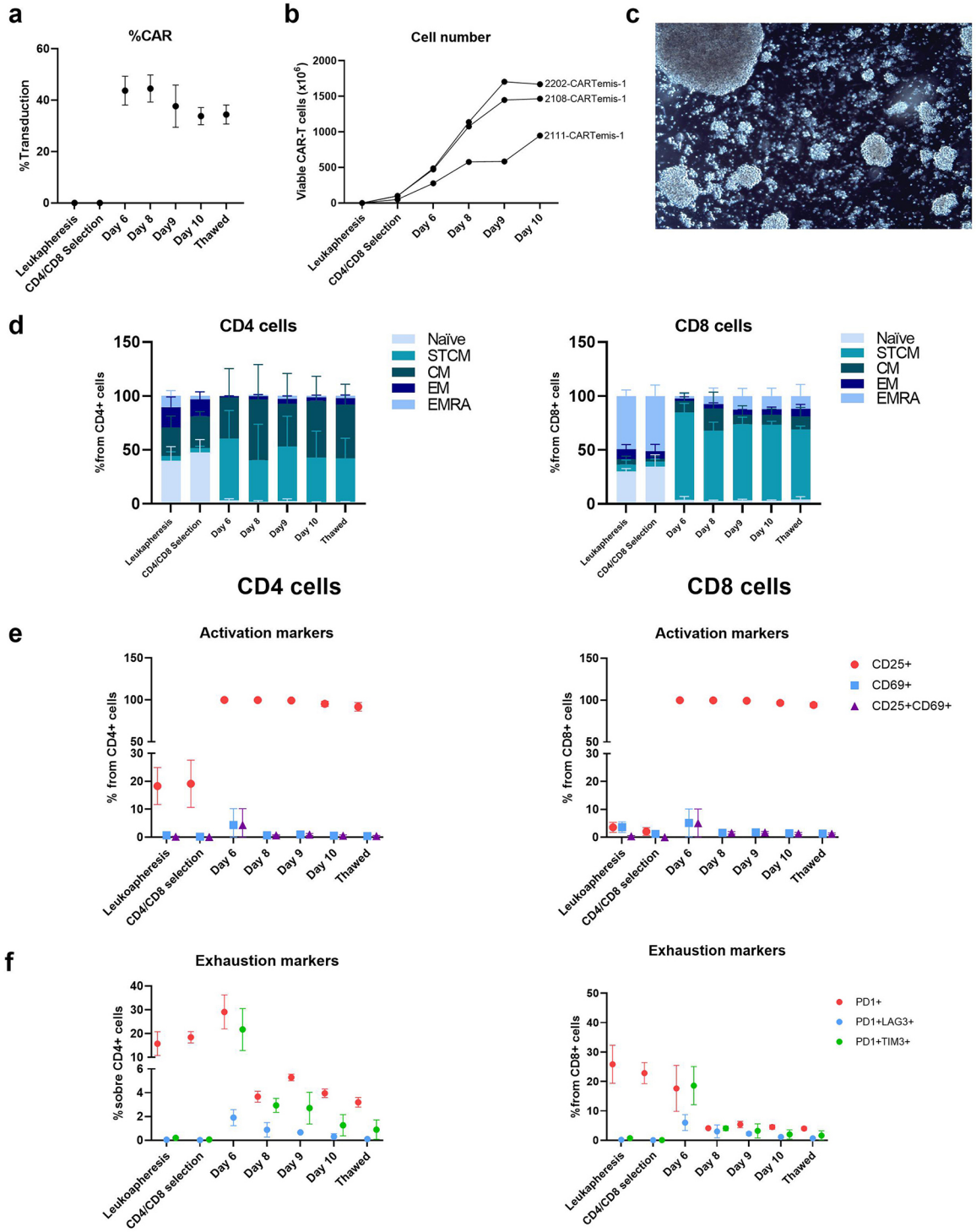

Fig. 4 CARTemis-1 cells can be generated at a clinical scale. CAR-T cell transduction, proliferation and immunophenotype were monitored throughout the manufacturing process. **a** Percentage of CAR+cells from T cells was analyzed by flow cytometry along the manufacturing process. **b** CAR+cell number from three independent healthy donors was quantified throughout the manufacturing process to confirm CAR-T cell expansion *ex vivo*.**c** Image depicting CARTemis-1 cells cluster formation in the CliniMACs Prodigy platform. **d** T cell subsets of CD4+ *(left)* and CD8+ *(right)* CARTemis-1 cells were analyzed at different time points of the manufacturing process. Activation **e** and exhaustion **f** markers of CD4+ *(left)* and CD8+ *(right)* CARTemis-1 cells were analyzed at different time points of the manufacturing process. Depicted are mean values of three independent lots produced + standard deviation

was also studied, and high levels of CD25 expression were observed in all donors at the final product in the CD4+ and CD8+ compartments (Fig. 4e). T-cell exhaustion was analyzed from leukapheresis to cryopreservation of the CARTemis-1 product. Levels of PD-1/TIM-3 increased with T-cell transduction and gradually decreased in the final product in CD4+ and CD8+ cells (Fig. 4f).

Preclinical and clinical CARTemis-1 products were compared according to cell viability, cell purity (T cells, monocytes, B cells, NK cells), CD4/CD8 ratio, and T-cell memory populations. Cell viability was similar, with a mean of 90.06% in the preclinical product and a mean of 85.77% in the clinical CARTemis-1 product (Supplementary Fig. 10a) ($p > 0.9999$). The preclinical CD4+/CD8 + T-cell ratio was 2.07, and the clinical CARTemis-1 product showed 1.87 CD4+/CD8+ ratio (Supplementary Fig. 10b) ($p = 0.21$). Cell composition was similar between both products, with > 95% T cells and 1–2% NKT cells in the final product (Supplementary Fig. 10c). TSCM in the preclinical and clinical products were also present at similar levels (Supplementary Fig. 10d). Regulatory T-cells (Tregs) were identified in the clinical CARTemis-1 product with a mean of 1.44% of CD4+ CD25+ CD127-FOXP3+ on day 10 of expansion (Supplementary Fig. 10e).

3.5 CARTemis-1 produced under GMP conditions shows potent and selective antitumor efficacy against MM cell lines and primary myeloma cells

CARTemis-1 produced under GMP conditions was cocultured with different MM cell lines (MM.1S and OPM-2) to measure antitumor efficacy at different time points during the manufacturing process. Antitumor efficacy was similar in all products obtained and comparable at the different time points measured (days 8, 9, and 10 postactivation) (Fig. 5a). As the antitumor efficacy was comparable at all time points and achieved the release criteria (Table 1) in all lots, the manufacturing protocol was considered optimal after 8 to 10 days of ex vivo expansion. Additionally, GMP-produced CARTemis-1 cells were cocultured with bone marrow-isolated primary myeloma cells from MM patients ($n = 3$) at an E: T ratio of 10:1 and showed potent antitumor efficacy (Fig. 5b and Supplementary Fig. 11). In addition, CARTemis-1 cells were generated from the T cells of MM patients and cocultured with myeloma cells at different E: T ratios, which demonstrated potent cytolytic activity (Fig. 5c). CAR-T cell potency of the final product was also measured by performing serial dilutions of the product with nonmodified T cells and analyzing the antitumor efficacy. A value of 10% was defined as the minimal CAR-T cell transduction required to achieve a specific tumor lysis of ≥ 20% (Fig. 5d). CARTemis-1 cells were also cocultured with MM cell lines to measure the specific production of antitumor cytokines. CARTemis-1 specifically produced IFN-γ and IL-2 when encountering BCMA+ cell lines. GM-CSF, a cytokine related to the most common side effect caused by CAR T cells (cytokine release syndrome, CRS), was also produced only in the presence of BCMA+ cells but to a significantly lesser extent (Fig. 5e).

CARTemis-1 cells were cryopreserved after 10 days of ex vivo expansion, and cell count, and antitumor efficacy were measured up to one year after cryopreservation to study the stability of the final product. The number of viable CAR-T cells was maintained for up to 12 months after cryopreservation, with a variability of < 20% (Supplementary Fig. 12a). Cell viability was maintained for up to 12 months after cryopreservation in the three clinical GMP-manufactured products and was > 70% (Supplementary Fig. 12b). CAR-T cell transduction was similar in all lots at all time points measured (Supplementary Fig. 12c). Antitumor efficacy was measured against MM cell lines and the release criteria (> 20% specific lysis at a 10:1 E: T ratio) were met for all three manufacturing processes at all time points measured and for up to 12 months after cryopreservation (Supplementary 12d). These results allowed our final cryopreserved products to be stored in vapor phase nitrogen for at least 12 months. Additional studies are being conducted over longer periods (24 months).

3.6 CARTemis-1 has a potent antitumor effect in mouse models with no signs of GvHD or tissue damage

In vitro coculture studies were performed to study the toxicity of CARTemis-1 against nonhematological tissues. Nonhematological cell lines from the lung, kidney, brain, liver, and breast were cocultured in the presence of CARTemis-1 or control nonmodified T-cells, and viability was measured by flow cytometry. No significant differences were observed between CARTemis-1 or control nonmodified T-cells (Fig. 6a). In vivo tissue damage was analyzed in NSG mice after CARTemis-1 ($n = 6$) or control nonmodified T-cell ($n = 4$) infusion in the absence of tumor cells. The presence of CARTemis-1 and nonmodified T-cells was confirmed in blood 3 days postinoculation (Fig. 6b). At the end of the experiment (day 10 postinoculation), we analyzed the infiltration of CARTemis-1 and nonmodified T-cells in spleen by flow cytometry to study the presence of infused T-cells in an in vivo model without tumor cells (Fig. 6c). Interestingly, an increase in spleen infiltration was observed in mice infused with control nonmodified T-cells as compared to those infused with CARTemis-1 cells ($p = 0.0095$). Tissue damage in the brain, cerebellum, intestine, lung, endometrium, ovary, testicle, spleen, and liver was analyzed

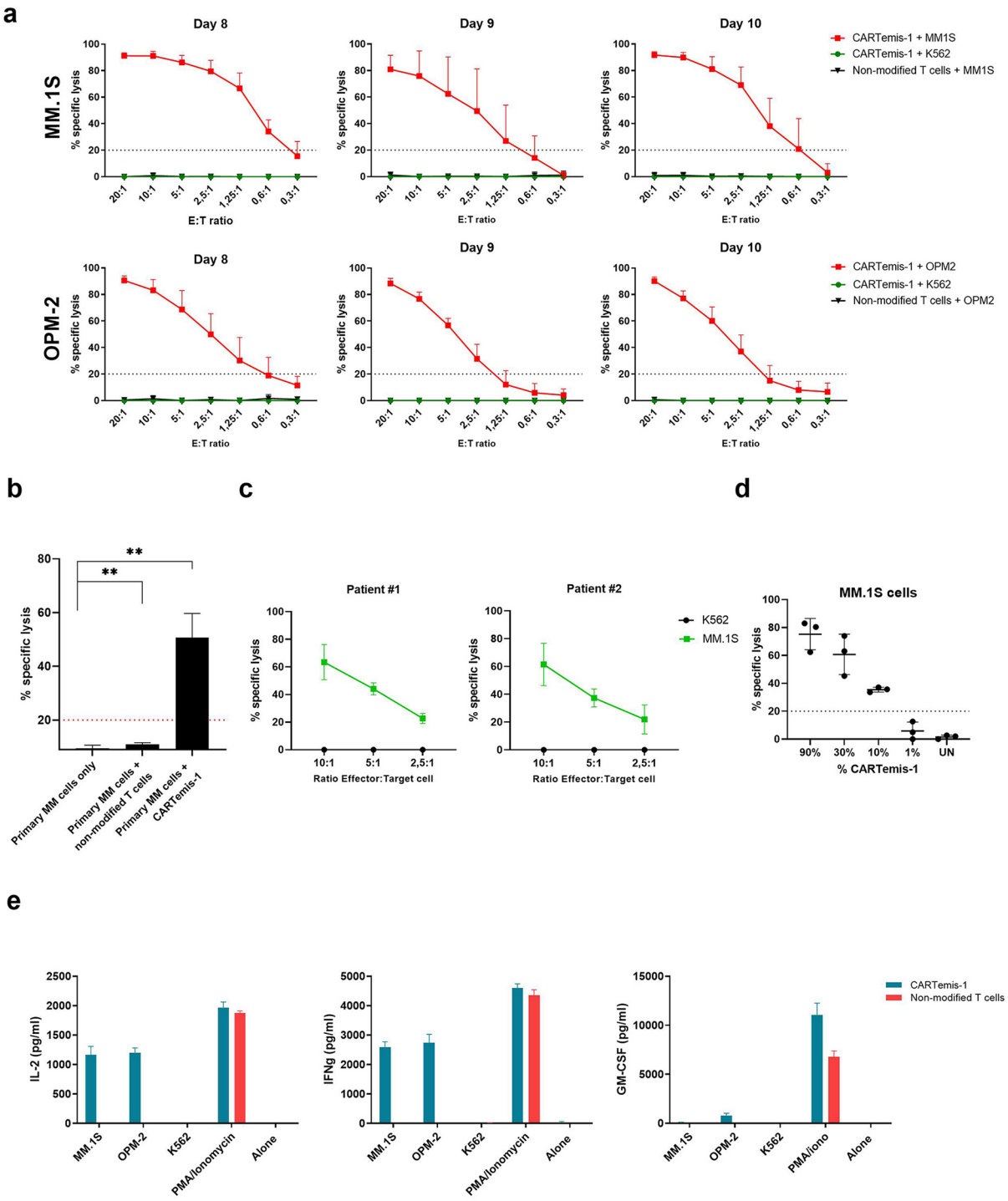

Fig. 5 CARTemis-1 clinical product shows a potent antitumoral effect *ex vivo*.**a** CARTemis-1 cells show potent and comparable specific cell lysis at different time points along the manufacturing process against two different BCMA+ myeloma cell lines (MM.1S, *top*, and OPM-2, *bottom*). **b** CARTemis-1 cells show potent antitumor cytotoxicity against primary myeloma cells at 24 h post-coculture. **c** CARTemis-1 cells generated from T cells derived from myeloma patients show potent specific cell lysis at 24 h post-coculture. **d** CARTemis-1 antitumor potency against MM.1S cells was analyzed by diluting the percentage of CAR + cells with non-modified T cells at 24 h post-coculture. **e** Cytokine release of IL-2 *(left)*, IFN-γ *(center)* and GM-CSF *(right)* of CARTemis-1 cells against BCMA+ myeloma cells was measured at 24 h post-coculture. Assay was performed in triplicate wells with 5,000 target cells per well ($n = 3$ biological replicates). Data show mean values of one representative experiment out of three independent lots produced + standard deviation. *P*-values between the indicated groups were calculated using unpaired T-test. $*p < 0.05$ $**p < 0.01$

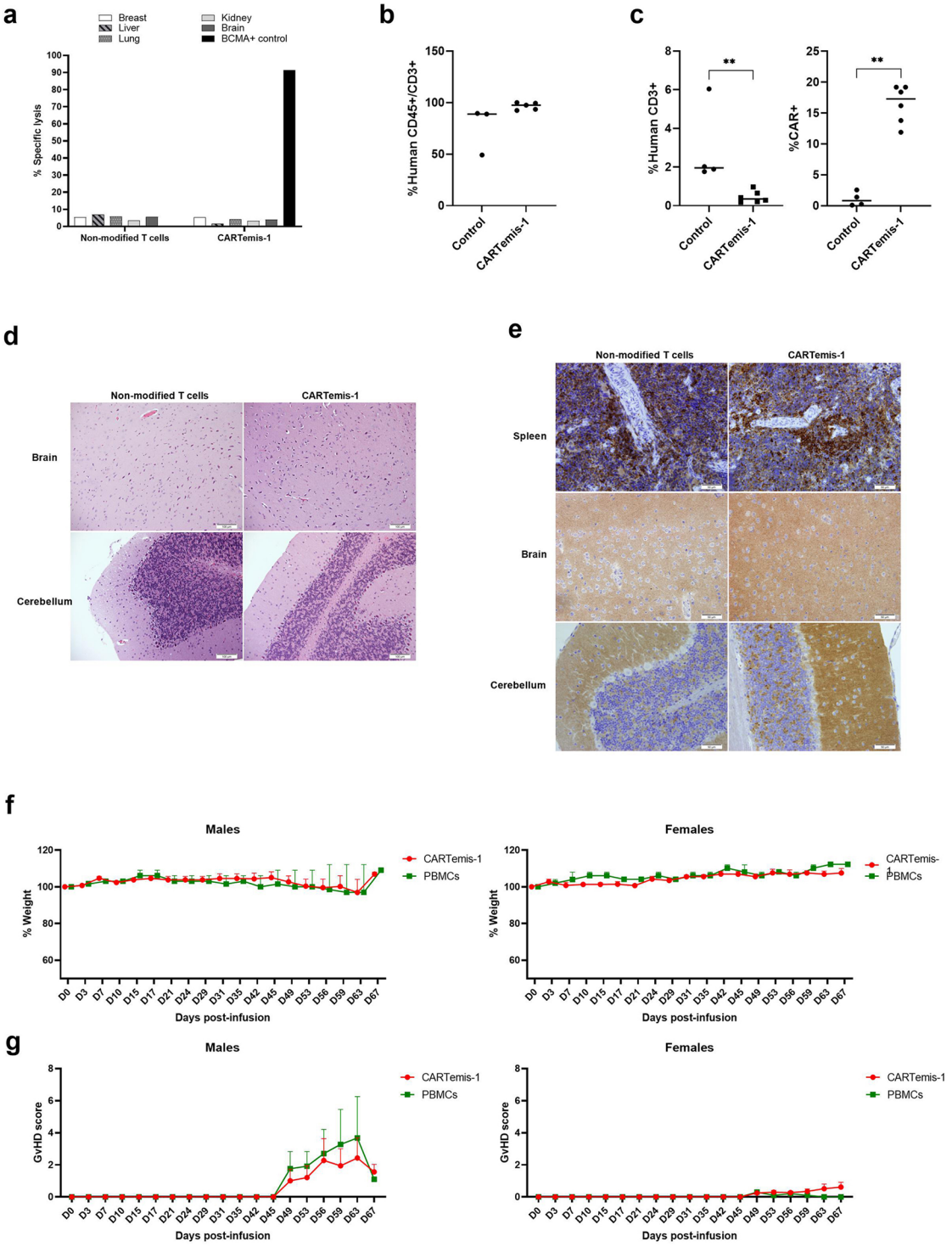

Fig. 6 CARTemis-1 cells do not induce tissue damage or increase GvHD incidence in NSG mice. **a** Cell viability of non-malignant cell lines cocultured with either control non-modified T cells or CARTemis-1 cells in vitro for 24 h was measured by flow cytometry. **b** Percentage of human CD45+ cells in blood of NSG mice after 3 days of inoculation of control non-modified T cells or CARTemis-1. **c** Infiltration of control non-modified T cells or CARTemis-1 cells in spleen 10 days post-inoculation. **d** Hematoxylin/eosin staining images of the brain *(top)* and cerebellum *(bottom)* of NSG mice 10 days post-inoculation of control non-modified T cells or CARTemis-1. **e** Immunohistochemistry staining of human CD3 + infiltration in brain *(top)* or cerebellum *(bottom)* of NSG mice 10 days post-inoculation of control non-modified T cells or CARTemis-1. Spleen was used as positive control *(left)*.**f** Percentage of weight loss of NSG mice post-inoculation of control non-modified T cells or CARTemis-1. **g** Acute GvHD score in NSG mice postinoculation of control non-modified T cells or CARTemis-1.

by immunohistopathology. Preserved tissue structure without relevant morphological alterations was observed in all tissues and samples studied after CARTemis-1 or control nonmodified T cell infusion (Fig. 6d). The spleen was used as a positive control (Fig. 6e, *top*). Infiltration of CARTemis-1 cells in the liver, lung, large intestine, endometrium, and ovary, was $<1\%$ (data not shown). No CARTemis-1 cells were found in the brain or cerebellum (Fig. 6e, *bottom*). Finally, we generated a third mouse model to study the incidence of GvHD. The incidence of GvHD in NSG mice after CARTemis-1 ($n=10$) or PBMC ($n=4$) inoculation was monitored for 67 days. No significant differences were observed in the incidence of GvHD between mice receiving CARTemis-1 and those receiving PBMCs according to body weight (Fig. 6f) or acute GvHD score (Fig. 6g). Notably, from day 45 postinoculation, we observed an increase in acute the GvHD score in males in both CARTemis-1 and PBMCs groups, suggesting that the reactivity was not related to CARTemis-1 infusion.

4 Discussion

Despite the impressive results of CAR-T cell therapy in MM, approximately 45% of patients relapse at 24 months of treatment according to the CARTITUDE-4 trial [5]. Several limitations have been identified and CAR construct optimization is under investigation. Here, we present the preclinical and clinical validation of a next-generation BCMA CAR-T cell (CARTemis-1).

The connecting sequence between the recognition domain to the transmembrane domain can profoundly affect CAR T-cell function by altering the length and flexibility of the resulting CAR [11]. According to these findings, previous studies have shown that the length of the CAR construct should be adapted to the specific target antigen to optimize antigen binding [11, 12]. In this regard, several studies have shown that the optimal spacer length depends on the distance of the targeted epitope from the tumor cell membrane [13–15]. Our study provides another example of how CAR flexibility can be modulated with different extracellular spacers to increase antitumor efficacy. In our study, CARTemis-1 with a longer spacer region, showed increased production of antitumor cytokines and increased cytotoxicity against myeloma cells. This is in accordance with previous studies in which longer spacers provided flexibility to the CAR and allowed for better access to membrane-proximal epitopes [11, 13, 14]. In this regard, CARTemis-1 recognizes a membrane-proximal epitope (24–41 AA) of the extracellular domain of BCMA. In addition, the extracellular domain of BCMA is very short (54 AA, UniProt: A7KBT6) compared to that of other proteins (CD19: 272 AA, UniProt: P15391; CD20: 668 AA, UniProt: P11836), suggesting that the long spacer of CARTemis-1 offers better flexibility to access the target.

In MM, BCMA is the preferred antigen due to its specific expression in plasma cells, with minimal expression in hematopoietic stem cells and normal tissues [16, 17]. However, the BCMA extracellular domain can be shed by the protease γ-secretase, and a soluble form of BCMA protein is secreted into the blood. This fact is one of the limitations of current anti-BCMA CAR-T therapy and is related to the loss of CAR-T efficacy [18–22]. In fact, some studies have shown increased levels of sBCMA in the serum of patients who do not respond to anti-BCMA CAR-T therapy [23, 24]. Multiple studies have demonstrated how increased levels of soluble BCMA affect the antitumor efficacy of BCMA CAR-T cells [18–20, 25]. Titration assays with recombinant soluble BCMA protein showed that CAR-T cell activity was inhibited at concentrations up to 32 ng/mL of BCMA [18]. Additionally, sBCMA at just 10 ng/mL significantly reduced IFN-γ secretion and cell cytotoxicity. Physiological amount of sBCMA in the serum of MM patients was also measured, finding it to be around 100 ng/mL [18]. In Lee et al., the performance of anti-BCMA CAR and anti-BCMA bispecific T cell engagers was also affected by sBCMA in a dose dependent manner effectively competing with the BCMA protein present in OPM-2 or K562/BCMA+ cells [26]. In contrast, CARTemis-1 demonstrated resistance to sBCMA up to 150 ng/mL in both in vitro and in vivo experiments (Figs. 1 and 2). Depending on the epitope recognized by the anti-BCMA CAR, sBCMA may interfere with the recognition of membrane-bound BCMA on myeloma cells and diminish anti-myeloma reactivity. One possible explanation is that the target epitope of soluble sBCMA may be inaccessible as sBCMA forms homodimeric or heterodimeric complexes. Previous studies have shown that sBCMA form large complexes with APRIL (a proliferation-inducing ligand) and BAFF (B-cell activating factor), suggesting that the epitope might be concealed within these complexes, thereby not impacting the functionality of BCMA CARs [27, 28]. Overall, CARTemis-1 has been rationally designed to enhance antitumor efficacy and we did not observe reduced antimyeloma reactivity from T cells expressing this BCMA-CAR in the presence of sBCMA.

To achieve adequate CAR-T cell doses, different protocols have been explored for ex-vivo expansion [29]. IL-2 is the most widely used cytokine for T-cell activation and expansion; however, several studies have explored other combinations in anti-CD19 CAR-T cells [30–33]. Limited information on the comparison between different expansion protocols has been described within anti-BCMA CAR products. These cytokines play pivotal roles in T-cell function. IL-2 induces TCR-activated T-cell proliferation,

but excessive levels can lead to antigen-induced cell death (AICD) [34]. Notably, IL-2 is a key contributor to Treg proliferation. This population has recently become relevant in the field, as an increased proportion of CAR-Tregs (> 5% CAR-Tregs) in infusion products has been correlated with a lower probability of response [35, 36]. IL-7, which is vital for T-cell homeostasis, maintains naïve and memory-resting T-cells, enhancing survival through the PI3KCLO-AKT pathway and increasing the expression of antiapoptotic factors [37, 38]. IL-15 supports memory T-cell proliferation and survival. IL-15 stimulation reduces mTORC1 activity, shifts T-cell metabolism to favor long-lived memory T-cells, increases less-differentiated CAR-T cells, enhances cell survival, and reduces exhaustion marker expression, which is correlated with heightened antitumor responses [39, 40]. However, while IL-15 stimulation has been reported to increase Treg accumulation in vitro [41], the concentration used in that study was up to 10 times higher than what we used for CARTemis-1 expansion. As a result, the proportion of Tregs in our CARTemis-1 product was minimal, averaging 1.44%. On the contrary, IL-2 is critical for Treg survival and functions as a key growth factor for these cells due to their high expression of the high-affinity IL-2 receptor CD25 [42–44]. Therefore, the combination of IL-7 and IL-15 is less likely to increase Treg percentages compared to IL-2. Taken altogether, these studies of CD19 CAR-T cells, are in accordance with the preclinical and clinical findings on our BCMA CAR product, in which the combination of IL-7 and IL-15 during the manufacturing process increased T-cell expansion and allowed the generation of less-differentiated and less exhausted CARTemis-1 cell products, maintaining hallmarks of T cell activation.

In addition to stimulating cytokines, cell culture period is a critical aspect of CAR-T cell therapy. Patients included in CAR-T cell therapy clinical trials are generally heavily pretreated [29]. Short cell culture periods (3–5 days) have been described [45–47]. However, this short ex vivo expansion may not be suitable for heavily pretreated patients with reduced and dysfunctional T cells [48]. In the present study, we characterized CARTemis-1 cells during the manufacturing process to define the optimal cell culture period. Although CAR-T cell dose was achieved on day 6 postactivation for the three GMP-validation processes, we observed CARTemis-1 cells exhibited increased overexpression of coinhibitory markers early post-transduction (day 4 post-transduction = day 6 postactivation) and that this exhausted phenotype decreased at days 8–10 postactivation, both at preclinical and clinical scales (Fig. 4f). Some recent studies have reported the feasibility of generating CAR-T cells in 22–36 h (FasT CAR-T) [49]; however, we demonstrated that early after T cell transduction, coinhibitory marker levels are significantly increased and therefore, at that time, the fitness of the product may not be optimal, particularly considering that some studies have reported that increased expression of coinhibitory markers in the infusion product is associated with worse outcomes [50–53]. In the present study, we propose from day 8 on as the optimal release time point for obtaining the best-fit CARTemis-1 product (days 8–10). In this sense, in addition to obtaining a sufficient CAR-T cell dose for infusion, monitoring the immunophenotype of the product during the manufacturing process may also be an important criterion to determine the optimal product.

Several limitations exist when generating patient-derived CAR-T cells for myeloma patients. First, obtaining sufficient T cells may be challenging because patients are often lymphopenic and have dysfunctional T cells [54]. Second, the characteristics of the leukapheresis material also have an impact on CAR-T cell fitness [55]. Finally, the number of prior treatments [56], patient age [57, 58], and the disease itself [32, 59] have been associated with limitations in the number and quality of CAR-T products. To overcome these limitations, we propose the possibility of generating CARTemis-1 cells from the small proportion of MM patients who undergo allogeneic stem cell transplantation (STC) and relapse after transplantation. However, this approach may present some drawbacks, such as the potential risk of inducing GvHD. Previous studies have analyzed the incidence of GvHD in patients receiving CAR-T cell therapy postallogeneic stem cell transplantation and found no increase in the incidence of GvHD [55, 60–63]. Despite the absence of clinical results with CARTemis-1 at this point, our mouse models suggest that CARTemis-1 cells would not increase GvHD incidence compared to PBMCs, despite the high levels of activation. In summary, CARTemis-1 might also be used for the treatment of the small subset of high-risk MM patients undergoing allo-SCT, which are clearly underrepresented in clinical trials.

Recently, the FDA reported the detection of T cell malignancies, including CAR-T-cell-positive lymphoma, in patients receiving commercially available CAR-T cell products [64]. Although the overall benefits of these products outweigh the potential risks, several international scientific experts have appointed the requirement for long-term follow-up in post monitorization studies to unravel the possible causal link between CAR-T therapy and these rare cases of T-cell malignancy [65]. In this sense, we have also incorporated a safety-gene consisting of the truncated epidermal growth factor receptor (EGFRt), which allows both the in vivo monitoring of CARTemis-1 using anti-EGFR antibodies and the elimination of CAR-T cells in vivo with cetuximab, an anti-EGFR antibody approved for use in the clinical setting.

5 Conclusions

In conclusion, despite the outstanding results of CAR-T cell therapy in R/R MM patients, the absence of a plateau and the ultimate relapse of patients are common to all trials. Here, we present the validation of a novel rationally designed academic BCMA CAR-T that shows enhanced antitumor efficacy and resistance to sBCMA inhibition. In addition, CARTemis-1 incorporates the expression of a safety-gene. Furthermore, we focused on analyzing the impact of the manufacturing process on the dynamics of CAR-T features, highlighting the importance of immunophenotypic characterization of CAR-T cells throughout the manufacturing process to correctly define the optimal cell culture protocol and expansion time to improve CAR-T cell product fitness and efficacy.

Supplementary Information The online version contains supplementary material available at https://doi.org/10.1007/s13402-024-00984-0.

Acknowledgements The authors thank the HUVR-IBiS Biobank (Andalusian Public Health System Biobank and ISCIII-Red de Biobancos y Biomodelos-PT20/00069) for the assessment and technical support provided.

Author contributions B.S.M. designed and performed experiments, analyzed data, and wrote the manuscript. V.E.G., L.P.O., P.H.D., and E.G.G. contributed in the GMP-production of CARTemis-1. B.G.A., P.H.D., M.R.G. and M.L.C. contributed to the in vitro characterization of CARTemis-1 and data analysis. J.L.R.O. helped in the sample collection. L.S.-F. contributed to the data analysis. B.A.A., M.A.M.A., and G.C. performed the quality controls of the GMP-productions of CARTemis-1. M.J.R. performed the immunohistopathology evaluation of the in vivo biodistribution study. T.C.V. contributed to data analysis. J.B., H.E. and M.H. served as scientific advisors and reviewed the manuscript. J.A.P.S. and E.G.G. designed experiments and project and critically reviewed the manuscript. All authors reviewed the manuscript.

Funding BGA has been supported by Instituto de Salud Carlos III (ISCIII) (PFIS-FI21/00222). MLC has been supported by the Consejería de Salud y Familias (CSyF)-Junta de Andalucía (RH*-0042-2020). LSF has been supported by the Instituto de Salud Carlos III (ISCIII) (Contrato Sara Borrell-CD21/00162). EGG has been supported by the Consejería de Universidad, Investigación e Innovación-Junta de Andalucía (DOC_01652) and by the Instituto de Sallud Carlos III (ISCIII) (Contrato Miguel Servet CP23/00139). This work has been supported by the Instituto de Salud Carlos III (ISCIII), Project RD21/0017/0021, Project ICI20/0118, and Project PI20/01792 by the Redes de Investigación Cooperativa Orientadas a Resultados en Salud (RICORS)-TERAV funded by European Union-NextGenerationEU. "Plan de Recuperación Transformación y Resiliencia"; and by the Ministerio de Ciencia e Innovación Project EQC2019-006475-P.

Data availability The data generated in this study are available upon request to the corresponding author.

Declarations

Ethics approval and consent to participate Peripheral blood mononuclear cells (PBMCs) were obtained from buffy coats of healthy donors kindly donated by the Regional Centre for Blood Transfusions at Virgen del Rocío University Hospital, Sevilla (Spain) after written informed consent. Leukapheresis from healthy donors were obtained from the leukapheresis unit of the Virgen del Rocío University Hospital, Sevilla (Spain) after written informed consent. Bone-marrow samples from patients with multiple myeloma were obtained from HUVR-IBiS Biobank at Hospital Virgen del Rocío after written informed consent. The University of Würzburg Institutional Animal Care and Use Committee and the Institutional Animal Care and Use Committee at Institute of Biomedicine in Seville approved all animal procedures.

Consent for publication All authors consent for publication.

Competing interests JAPS is an advisor or consultant for Novartis, Janssen, Roche, Jazz Pharmaceuticals, Amgen, and Gilead Sciences; reports research support from Novartis, Janssen, Pfizer, Roche, and Takeda; reports travel support from Roche, Gilead Sciences and Janssen; and reports patents, royalties, or other intellectual property from Entourage Bioscience on cannabinoid derivatives. EGG has been a consultant to Cellgene and GLS, and received travel grants and/or speaker fees from Cellgene, Amgen, Janssen. EGG and MH are co-inventors on a patent application on the use of BCMA-CAR T-cell therapy in combination with ATRA, "Combination treatment of BCMA CAR-T and ATRA in multiple myeloma" (WO2021/209498 A1), that has been filed by the University of Würzburg, Würzburg, Germany and licensed to T-CURX GmbH, Würzburg, Germany.

References

1. N.C. Munshi, L.D. Anderson, N. Shah, D. Madduri, J. Berdeja, S. Lonial et al., Idecabtagene vicleucel in relapsed and refractory multiple myeloma. N. Engl. J. Med. **384**(8), 705–716 (2021)
2. T. Martin, S.Z. Usmani, J.G. Berdeja, M. Agha, A.D. Cohen, P. Hari et al., Ciltacabtagene autoleucel, an anti–B-cell maturation antigen chimeric antigen receptor T-cell therapy, for relapsed/refractory multiple myeloma: CARTITUDE-1 2-year follow-up. J. Clin. Oncol. (2022)
3. J.G. Berdeja, D. Madduri, S.Z. Usmani, A. Jakubowiak, M. Agha, A.D. Cohen et al., Ciltacabtagene autoleucel, a B-cell maturation antigen-directed chimeric antigen receptor T-cell therapy in patients with relapsed or refractory multiple myeloma (CARTITUDE-1): a phase 1b/2 open-label study. Lancet. **398**(10297), 314–324 (2021)

4. B. Dhakal, K. Yong, S.J. Harrison, M.V. Mateos, P. van de Moreau et al., First phase 3 results from CARTITUDE-4: cilta-cel versus standard of care (PVd or DPd) in lenalidomide-refractory multiple myeloma. **41**(17_suppl), LBA106–LBA106 (2023). https://doi.org/10.1200/JCO.2023.41.17_suppl.LBA106
5. J. San-Miguel, B. Dhakal, K. Yong, A. Spencer, S. Anguille, M.V. Mateos et al., Cilta-cel or standard care in lenalidomide-refractory multiple myeloma. N. Engl. J. Med. (2023). https://doi.org/10.1056/NEJMoa2303379
6. K. Rejeski, M.D. Jain, E.L. Smith, Mechanisms of resistance and treatment of relapse after CAR T-cell therapy for large B-cell lymphoma and multiple myeloma. (2023). https://doi.org/10.1016/j.jtct.2023.04.007
7. L.D. Anderson, B. Dhakal, T. Jain, O.O. Oluwole, G.L. Shah, S. Sidana et al., Chimeric antigen receptor T cell therapy for myeloma: where are we now and what is needed to move chimeric antigen receptor T cells forward to earlier lines of therapy? Expert panel opinion from the American Society for Transplantation and Cellular Therapy. Transpl. Cell. Ther. (2023)
8. E. García-Guerrero, B. Sierro-Martínez, J.A. Pérez-Simón, Overcoming chimeric antigen receptor (CAR) modified T-cell therapy limitations in multiple myeloma. Front. Immunol. **11** (2020). https://pubmed.ncbi.nlm.nih.gov/32582204/
9. S. Hipp, Y.T. Tai, D. Blanset, P. Deegen, J. Wahl, O. Thomas et al., A novel BCMA/CD3 bispecific T-cell engager for the treatment of multiple myeloma induces selective lysis in vitro and in vivo. Leukemia. **31**(8), 1743–1751 (2017). https://pubmed.ncbi.nlm.nih.gov/28025583/
10. C.E. Brown, C.L. Wright, A. Naranjo, R.P. Vishwanath, W.C. Chang, S. Olivares et al., Biophotonic cytotoxicity assay for high-throughput screening of cytolytic killing. J. Immunol. Methods. **297**(1–2), 39–52 (2005)
11. R.D. Guest, R.E. Hawkins, N. Kirillova, E.J. Cheadle, J. Arnold, A. O'Neill et al., The role of extracellular spacer regions in the optimal design of chimeric immune receptors: evaluation of four different scFvs and antigens. J. Immunother. **28**(3), 203–211 (2005). https://journals.lww.com/immunotherapy-journal/fulltext/2005/05000/the_role_of_extracellular_spacer_regions_in_the.5.aspx
12. M. Hudecek, D. Sommermeyer, P.L. Kosasih, A. Silva-Benedict, L. Liu, C. Rader et al., The nonsignaling extracellular spacer domain of chimeric antigen receptors is decisive for in vivo antitumor activity. Cancer Immunol. Res. **3**(2), 125–135 (2015). https://aacrjournals.org/cancerimmunolres/article/3/2/125/467742/The-Nonsignaling-Extracellular-Spacer-Domain-of
13. S.E. James, P.D. Greenberg, M.C. Jensen, Y. Lin, J. Wang, B.G. Till et al., Antigen sensitivity of CD22-specific chimeric TCR is modulated by target epitope distance from the cell membrane. J. Immunol. **180**(10), 7028–7038 (2008). https://doi.org/10.4049/jimmunol.180.10.7028
14. S. Guedan, H. Calderon, A.D. Posey, M.V. Maus, Engineering and design of chimeric antigen receptors. Mol. Ther. Methods Clin. Dev. **12**, 145–156 (2019). http://www.cell.com/article/S2329050118301335/fulltext
15. G. Dotti, S. Gottschalk, B. Savoldo, M.K. Brenner, J. Carl, Design and development of therapies using chimeric antigen receptor-expressing T cells. Immunol. Rev. **257** (2013). www.immunologicalreviews.com
16. N. Shah, A. Chari, E. Scott, K. Mezzi, S.Z. Usmani, B-cell maturation antigen (BCMA) in multiple myeloma: rationale for targeting and current therapeutic approaches. Leukemia. **34**(4), 985–1005 (2020). https://www.nature.com/articles/s41375-020-0734-z
17. R.O. Carpenter, M.O. Evbuomwan, S. Pittaluga, J.J. Rose, M. Raffeld, S. Yang et al., B-cell maturation antigen is a promising target for adoptive T-cell therapy of multiple myeloma. Clin. Cancer Res. **19**(8), 2048–2060 (2013). https://aacrjournals.org/clincancerres/article/19/8/2048/208469/B-cell-Maturation-Antigen-Is-a-Promising-Target
18. L. Perez-Amill, G. Suñe, A. Antoñana-Vildosola, M. Castella, A. Najjar, J. Bonet et al., Preclinical development of a humanized chimeric antigen receptor against B-cell maturation antigen for multiple myeloma. Haematologica. **106**(1), 173 (2021). /pmc/articles/PMC7776337/.
19. S.A. Laurent, F.S. Hoffmann, P.H. Kuhn, Q. Cheng, Y. Chu, M. Schmidt-Supprian et al., γ-secretase directly sheds the survival receptor BCMA from plasma cells. Nat. Commun. (2015)
20. M.J. Pont, T. Hill, G.O. Cole, J.J. Abbott, J. Kelliher, A.I. Salter et al., γ-Secretase inhibition increases efficacy of BCMA-specific chimeric antigen receptor T cells in multiple myeloma. Blood. **134**(19), 1585–1597 (2019). https://ashpublications.org/blood/article/134/19/1585/374996/Secretase-inhibition-increases-efficacy-of-BCMA
21. E. Sanchez, A. Gillespie, G. Tang, M. Ferros, N.M. Harutyunyan, S. Vardanyan et al., Soluble B-Cell maturation antigen mediates tumor-induced immune deficiency in multiple myeloma. Clin. Cancer Res. **22**(13), 3383–3397 (2016). https://pubmed.ncbi.nlm.nih.gov/26960399/
22. H. Chen, M. Li, N. Xu, N. Ng, E. Sanchez, C.M. Soof et al., Serum B-cell maturation antigen (BCMA) reduces binding of anti-BCMA antibody to multiple myeloma cells. Leuk Res. **81**, 62–66 (2019). https://pubmed.ncbi.nlm.nih.gov/31035033/
23. Y. Shen, J. Liu, B. Wang, Y. Zhang, Y. Xu, X. Wang et al., Serum soluble BCMA can be used to monitor relapse of multiple myeloma patients after chimeric antigen receptor T-cell immunotherapy. Curr. Res. Transl Med. **71**(2), 103378 (2023)
24. K. Seipel, N. Porret, G. Wiedemann, B. Jeker, V.U. Bacher, T. Pabst, sBCMA plasma level dynamics and anti-BCMA CAR-T-cell treatment in relapsed multiple myeloma. Curr. Issues Mol. Biol. **44**(4), 1463 (2022). /pmc/articles/PMC9164019/.
25. A.J. Cowan, M.J. Pont, B.D. Sather, C.J. Turtle, B.G. Till, E.N. Libby et al., γ-Secretase inhibitor in combination with BCMA chimeric antigen receptor T-cell immunotherapy for individuals with relapsed or refractory multiple myeloma: a phase 1, first-in-human trial. Lancet Oncol. **24**(7), 811–822 (2023)
26. H. Lee, M. Durante, S. Ahn, N. Leblay, M. Poorebrahim, R. Maity et al., The impact of soluble BCMA and BCMA gain on anti-BCMA immunotherapies in multiple myeloma. Blood [Internet]. **142**(Suppl. 1), 4688–4688 (2023). https://doi.org/10.1182/blood-2023-188080
27. S.G. Hymowitz, D.R. Patel, H.J.A. Wallweber, S. Runyon, M. Yan, J.P. Yin et al., Structures of APRIL-receptor complexes: like BCMA, TACI employs only a single cysteine-rich domain for high affinity ligand binding. J. Biol. Chem. **280**(8), 7218–7227 (2005). https://pubmed.ncbi.nlm.nih.gov/15542592/
28. Y. Liu, X. Hong, J. Kappler, L. Jiang, R. Zhang, L. Xu et al., Ligand-receptor binding revealed by the TNF family member TALL-1. Nature. **423**(6935), 49–56 (2003). https://pubmed.ncbi.nlm.nih.gov/12721620/
29. N. Watanabe, F. Mo, M.K. McKenna, Impact of manufacturing procedures on CAR T cell functionality. Front. Immunol. **13** (2022). https://pubmed.ncbi.nlm.nih.gov/35493513/
30. Y. Rochman, R. Spolski, W.J. Leonard, New insights into the regulation of T cells by γc family cytokines. Nat. Rev. Immunol. **9**, 480–490 (2009)
31. A. Ma, R. Koka, P. Burkett, Diverse functions of IL-2, IL-15, and IL-7 in lymphoid homeostasis. Ann. Rev. Immunol. **24**, 657–679 (2006)
32. J.M. Hoffmann, M.L. Schubert, L. Wang, A. Hückelhoven, L. Sellner, S. Stock et al., Differences in expansion potential of naive chimeric antigen receptor T cells from healthy donors and untreated chronic lymphocytic leukemia patients. Front Immunol. **8**(Jan), 315028 (2018)

33. Y. Xu, M. Zhang, C.A. Ramos, A. Durett, E. Liu, O. Dakhova et al., Closely related T-memory stem cells correlate with in vivo expansion of CAR.CD19-T cells and are preserved by IL-7 and IL-15. Blood. **123**(24), 3750–3759 (2014)
34. M.J. Lenardo, lnterleukin-2 programs mouse αβ T lymphocytes for apoptosis. Nature. **353**(6347), 858–861 (1991). https://www.nature.com/articles/353858a0
35. Z. Good, J.Y. Spiegel, B. Sahaf, M.B. Malipatlolla, Z.J. Ehlinger, S. Kurra et al., Post-infusion CAR TReg cells identify patients resistant to CD19-CAR therapy. Nat. Med. **28**(9), 1860–1871 (2022). https://doi.org/10.1038/s41591-022-01960-7
36. N.J. Haradhvala, M.B. Leick, K. Maurer, S.H. Gohil, R.C. Larson, N. Yao et al., Distinct cellular dynamics associated with response to CAR-T therapy for refractory B cell lymphoma. Nat. Med. 28(9), 1848–1859 (2022). https://www.nature.com/articles/s41591-022-01959-0
37. K.S. Schluns, W.C. Kieper, S.C. Jameson, L. Lefrançois, Interleukin-7 mediates the homeostasis of naïve and memory CD8 T cells in vivo. Nat. Immunol. **1**(5), 426–432 (2000). https://www.nature.com/articles/ni1100_426
38. A.W. Goldrath, P.V. Sivakumar, M. Glaccum, M.K. Kennedy, M.J. Bevan, C. Benoist et al., Cytokine requirements for acute and Basal homeostatic proliferation of naive and memory CD8 + T cells. J. Exp. Med. **195**(12), 1515–1522 (2002). https://pubmed.ncbi.nlm.nih.gov/12070279/
39. D.A. RA, W.X.Y.D.W. JR CF, K, et al. IL15 Enhances CAR-T Cell Antitumor Activity by Reducing mTORC1 Activity and Preserving Their Stem Cell Memory Phenotype. Cancer Immunol. Res. **7**(5), 759–772 (2019). https://pubmed.ncbi.nlm.nih.gov/30890531/
40. J. Zhou, L. Jin, F. Wang, Y. Zhang, B. Liu, T. Zhao, Chimeric antigen receptor T (CAR-T) cells expanded with IL-7/IL-15 mediate superior antitumor effects. Protein Cell **10**, 764–769 (2019)
41. H. Imamichi, I. Sereti, H.C. Lane, IL-15 acts as a potent inducer of CD4 + CD25hi cells expressing FOXP3. Eur. J. Immunol. **38**(6), 1621–1630 (2008)
42. T.R. Malek, A. Yu, V. Vincek, P. Scibelli, L. Kong, CD4 regulatory T cells prevent lethal autoimmunity in IL-2Rbeta-deficient mice. Implications for the nonredundant function of IL-2. Immunity. **17**(2), 167–178 (2002). https://pubmed.ncbi.nlm.nih.gov/12196288/
43. A.M. Thornton, E.M. Shevach, CD4 + CD25 + immunoregulatory T cells suppress polyclonal T cell activation in vitro by inhibiting interleukin 2 production. J. Exp. Med. **188**(2), 287–296 (1998). https://pubmed.ncbi.nlm.nih.gov/9670041/
44. T.R. Malek, A.L. Bayer, Tolerance, not immunity, crucially depends on IL-2. Nat. Rev. Immunol. **4**(9), 665–674 (2004). https://www.nature.com/articles/nri1435
45. S. Ghassemi, S. Nunez-Cruz, R.S. O'Connor, J.A. Fraietta, P.R. Patel, J. Scholler et al., Reducing ex vivo culture improves the antileukemic activity of chimeric antigen receptor (CAR) T cells. Cancer Immunol. Res. **6**(9), 1100–1109 (2018). https://aacrjournals.org/cancerimmunolres/article/6/9/1100/468912/Reducing-Ex-Vivo-Culture-Improves-the-Antileukemic. Cited 15 Mar 2023
46. B. Engels, X. Zhu, J. Yang, A. Price, A. Sohoni, A.M. Stein et al., Preservation of T-Cell stemness with a Novel Expansionless CAR-T Manufacturing process, which reduces Manufacturing Time to Less Than two days, drives enhanced CAR-T cell efficacy. Blood. **138**(Suppl. 1), 2848–2848 (6377)
47. P.A. Lu, Feasibility, and *Safety Study of a Novel CD19-Directed Synthetic T-Cell Receptor and Antigen Receptor (STAR) T-Cell Therapy for Refractory and Relapsed (R/R) B Cell Acute Lymphoblastic Leukemia (B-ALL)* (ASH, 2020)
48. A. Schietinger, M. Philip, V.E. Krisnawan, E.Y. Chiu, J.J. Delrow, R.S. Basom et al., Tumor-specific T Cell dysfunction is a dynamic antigen-driven differentiation program initiated early during tumorigenesis. Immunity. **45**(2), 389–401 (2016). https://pubmed.ncbi.nlm.nih.gov/27521269/
49. J. Yang, J. He, X. Zhang, J. Li, Z. Wang, Y. Zhang et al., Next-day manufacture of a novel anti-CD19 CAR-T therapy for B-cell acute lymphoblastic leukemia: first-in-human clinical study. https://doi.org/10.1038/s41408-022-00694-6
50. J.A. Fraietta, S.F. Lacey, E.J. Orlando, I. Pruteanu-Malinici, M. Gohil, S. Lundh et al., Determinants of response and resistance to CD19 chimeric antigen receptor (CAR) T cell therapy of chronic lymphocytic leukemia. Nat. Med. **24**(5), 563–571 (2018). https://doi.org/10.1038/s41591-018-0010-1
51. Q. Deng, G. Han, N. Puebla-Osorio, M.C.J. Ma, P. Strati, B. Chasen et al., Characteristics of anti-CD19 CAR T cell infusion products associated with efficacy and toxicity in patients with large B cell lymphomas. Nat. Med. **26**(12), 1878–1887 (2020)
52. O.C. Finney, H. Brakke, S. Rawlings-Rhea, R. Hicks, D. Doolittle, M. Lopez et al., CD19 CAR T cell product and disease attributes predict leukemia remission durability. J. Clin. Invest. **129**(5), 2123–2132 (2019)
53. Y. Lin, N.S. Raje, J.G. Berdeja, D.S. Siegel, S. Jagannath, D. Madduri et al., Idecabtagene vicleucel for relapsed and refractory multiple myeloma: post hoc 18-month follow-up of a phase 1 trial. Nat. Med. **29**(9), 2286–2294 (2023)
54. S. Rafiq, C.S. Hackett, R.J. Brentjens, Engineering strategies to overcome the current roadblocks in CAR T cell therapy. Nat. Rev. Clin. Oncol. **17**(3), 147–167 (2019). https://www.nature.com/articles/s41571-019-0297-y
55. J.H. Park, I. Rivière, M. Gonen, X. Wang, B. Sénéchal, K.J. Curran et al., Long-term follow-up of CD19 CAR therapy in acute lymphoblastic leukemia. N. Engl. J. Med. **378**(5), 449–459 (2018). https://doi.org/10.1056/nejmoa1709919. https://www.nejm.org/doi/full/
56. N. Singh, J. Perazzelli, S.A. Grupp, D.M. Barrett, Early memory phenotypes drive T cell proliferation in patients with pediatric malignancies. Sci. Transl. Med. **8**(320) (2016). https://doi.org/10.1126/scitranslmed.aad5222. https://www.science.org/doi/
57. N. Salam, S. Rane, R. Das, M. Faulkner, R. Gund, U. Kandpal et al., T cell ageing: Effects of age on development, survival & function. Indian J. Med. Res. **138**(5), 595 (2013). /pmc/articles/PMC3928693/.
58. S. Palmer, L. Albergante, C.C. Blackburn, T.J. Newman, Thymic involution and rising disease incidence with age. Proc. Natl. Acad. Sci. U. S. A. **115**(8), 1883–1888 (2018). https://doi.org/10.1073/pnas.1714478115. https://www.pnas.org/doi/abs/
59. J.A. Fraietta, K.A. Beckwith, P.R. Patel, M. Ruella, Z. Zheng, D.M. Barrett et al., Ibrutinib enhances chimeric antigen receptor T-cell engraftment and efficacy in leukemia. Blood. **127**(9), 1117–1127 (2016). https://ashpublications.org/blood/article/127/9/1117/126450/Ibrutinib-enhances-chimeric-antigen-receptor-T
60. L. Hammons, S. Haider, M.C. Pasquini, S. Chhabra, S. Radhakrishnan, A.E. Zamora et al., Chimeric antigen receptor-T (CAR-T) cell therapy targeting BCMA in patients with prior allogeneic transplantation (allo-HCT) in relapsed and/or refractory multiple myeloma (RRMM). Blood. **140**(Suppl. 1), 7215–7216 (2022). https://ashpublications.org/blood/article/140/Supplement1/7215/493112/Chimeric-Antigen-Receptor-T-CAR-T-Cell-Therapy
61. J.N. Kochenderfer, M.E. Dudley, R.O. Carpenter, S.H. Kassim, J.J. Rose, W.G. Telford et al., Donor-derived CD19-targeted T cells cause regression of malignancy persisting after allogeneic hematopoietic stem cell transplantation. Blood. **122**(25), 4129–4139 (2013). https://ashpublications.org/blood/article/122/25/4129/32058/Donor-derived-CD19-targeted-T-cells-cause
62. F. Lutfi, N. Holtzman, J. Siglin, A. Bukhari, M. Mustafa Ali, D. Kim et al., Chimeric antigen receptor T-cell therapy after

allogeneic stem cell transplant for relapsed/refractory large B-cell lymphoma. Br. J. Haematol. **192**(1), 212–216 (2021)
63. J. Siglin, F. Lutfi, A. Bukhari, N.G. Holtzman, D.W. Kim, M.M. Ali et al., Pseudo-allogeneic CAR-T therapy after allogeneic stem cell transplantation in relapsed/refractory B-cell NHL. Blood. **136**(Suppl. 1), 22–23 (2020). https://ashpublications.org/blood/article/136/Supplement1/22/471006/Pseudo-Allogeneic-CAR-T-Therapy-after-Allogeneic
64. R. Nelson, FDA investigating safety risks in CAR T-cell recipients. Lancet. **402**(10418), 2181 (2023). http://www.thelancet.com/article/S0140673623027472/fulltext
65. B.L. Levine, M.C. Pasquini, J.E. Connolly, D.L. Porter, M.P. Gustafson, J.J. Boelens et al., Unanswered Questions Following Reports of Secondary Malignancies after CAR-T cell Therapy. Nat. Med. Nat. Res. (2024)